[CANCER RESEARCH 64, 9209–9216, December 15, 2004]

Androgen-Independent Prostate Cancer Is a Heterogeneous Group of Diseases: Lessons from a Rapid Autopsy Program

Rajal B. Shah,[1,3] Rohit Mehra,[1] Arul M. Chinnaiyan,[1,3] Ronglai Shen,[4] Debashis Ghosh,[4] Ming Zhou,[1] Gary R. MacVicar,[2] Soorynarayana Varambally,[1] Jason Harwood,[1] Tarek A. Bismar,[5] Robert Kim,[5] Mark A. Rubin,[5,6,7] and Kenneth J. Pienta[2,3]

Departments of [1]Pathology, [2]Medical Oncology, [3]Urology, and [4]Biostatistics, University of Michigan School of Medicine, Ann Arbor, Michigan; [5]Department of Pathology, Brigham and Women's Hospital, Boston, Massachusetts; [6]Department of Pathology, Dana Farber Cancer Institute, Boston, Massachusetts; and [7]Department of Pathology, Harvard Medical School, Boston, Massachusetts

ABSTRACT

Understanding the biology of prostate cancer metastasis has been limited by the lack of tissue for study. We studied the clinical data, distribution of prostate cancer involvement, morphology, immunophenotypes, and gene expression from 30 rapid autopsies of men who died of hormone-refractory prostate cancer. A tissue microarray was constructed and quantitatively evaluated for expression of prostate-specific antigen, androgen receptor, chromogranin, synaptophysin, MIB-1, and α-methylacylCoA-racemase markers. Hierarchical clustering of 16 rapid autopsy tumor samples was performed to evaluate the cDNA expression pattern associated with the morphology. Comparisons were made between patients as well as within the same patient. Metastatic hormone-refractory prostate cancer has a heterogeneous morphology, immunophenotype, and genotype, demonstrating that "metastatic disease" is a group of diseases even within the same patient. An appreciation of this heterogeneity is critical to evaluating diagnostic and prognostic biomarkers as well as to designing therapeutic targets for advanced disease.

INTRODUCTION

In the United States, prostate cancer remains the most common solid tumor malignancy in men, causing ~30,000 deaths in 2004 (1). With the goal of trying to better understand the biology of prostate tumorigenesis and metastasis, we have developed a rapid autopsy program to collect tumors from multiple sites including solid organs and bone to perform molecular studies to better delineate prostate cancer progression (2). Our group has used these samples with a combination of cDNA expression and tissue microarray analysis approaches to identify novel prostate cancer biomarkers, including Enhancer of Zeste homolog 2 (EZH2), Metastasis associated 1 (MTA1), PIM1, and α-methylacyl-CoA racemase (AMACR), with a supervised analysis comparing androgen-independent to localized prostate cancer samples (3–7).

These previous studies, however, lump metastatic tumors as a single entity, whereas the patterns of dissemination at autopsy suggest that metastatic cancer may better be characterized as a group of diseases rather than a single entity. Our goal of the present study was to study the phenotypic characteristics of metastatic prostate cancer in detail. Our data indicate that metastatic prostate cancer demonstrates substantial heterogeneity, even within the same patient. We believe detailed characterization of the heterogeneous phenotypic spectrum of end stage metastatic prostate cancer will guide future molecular studies on metastatic disease, as well as provide a framework for identifying subtypes that may respond better to novel therapeutics.

MATERIALS AND METHODS

Rapid Autopsy Tissue Procurement Protocol. The rapid autopsy program was approved by the Institutional Review Board of University of Michigan and supported by Specialized Program of Research Excellence in Prostate Cancer (National Cancer Institute grant CA69568) and the Prostate Cancer Foundation. Patients were identified with hormone-refractory prostate cancer by the Medical Oncology Service of the Comprehensive Cancer Center at the University of Michigan Hospitals as described previously (2). The clinical information obtained for each patient included age at diagnosis, age at death, months to death after diagnosis, initial Gleason score, time on hormonal therapy only, and type of primary and systemic therapy. These autopsies have been referred to as "rapid" or "warm" because of the short time interval (average 3 hours) between patient death and starting the autopsy.

Pathology Data. Pathology data included detailed histologic evaluation of prostate cancer at metastatic sites, location and systemic distribution pattern of metastasis at both osseous and nonosseous organ sites, and histology of the prostate in event of no previous radical prostatectomy. Microscopic evaluation of all slides from each tumor site was evaluated by the study pathologists (R. B. S., R. M., M. A. R.).

Construction of Tissue Microarray and Immunohistochemistry. A tissue microarray was constructed from all 30 autopsies to represent all of the prostate cancer metastasis sites and the prostate (if present). Three cores (0.6 mm in diameter) were taken from each representative tissue block. The tissue microarray construction protocol has been described previously (8–10). This tissue microarray was immunostained for a variety of tumor markers, including prostate-specific antigen (PSA), androgen receptor (AR), chromogranin (CGA), synaptophysin (SYN), α-methylacylCoA-racemase (AMACR), and the proliferation marker MIB-1. Immunohistochemistry was performed with standard avidin-biotin complex protocol. For PSA, CGA, SYN, AMACR and MIB-1 antibodies, antigen retrieval was performed in citrate buffer at pH 6.0; and for AR, antigen retrieval was performed with EDTA at pH 8.0 in a pressure cooker. The primary antibodies and dilution were as followings: polyclonal PSA (Dako Cytomation, Carpenteria, CA) 1:2000; monoclonal AR-clone AR 441 (NeoMarkers, Fremont, CA) 1:50; CGA (Biogenex, San Ramon, CA) 1:160; SYN (Biogenex) 1:600; AMACR (generated from denatured recombinant antigen to AMACR) 1:5000; and MIB-1 (Dako Corporation, Carpentaria, CA) 1:100. The slides were evaluated for adequacy with a standard bright field microscope. Digital images were then acquired with the BLISS Imaging System (Bacus Laboratory, Lombard, IL).

Immunohistochemistry evaluation was carried out with Chromavision ACIS II version (Chromavision Medical Systems, Inc., San Juan Capistrano, CA; refs. 11–13). The ACIS uses preprogrammed advanced color detection software that measures immunohistochemical stains intensity (range, 0–255) and percentage expression (0–100%). Because the system has no means of distinguishing tumor tissue from noncancerous tissue, all of the images were reviewed by one of the study pathologists (T. A. B.). Tumor tissue was electronically circled on the computer screen, and only those areas were used to measure the percentage of the circled cells that stained positive for each of

Received 7/14/04; revised 8/18/04; accepted 9/15/04.

Grant support: Supported by the Specialized Program of Research Excellence for Prostate Cancer (SPORE) National Cancer Institute (NCI) grant P50CA69568, NCI grant CA 97063 (A. Chinnaiyan and M. Rubin), R01AG21404 (M. Rubin and A. Chinnaiyan), American Cancer Society RSG-02-179-MGO (A. Chinnaiyan and M. Rubin), and NCI CA102872 (K. Pienta). K. Pienta is supported by the American Cancer Society as a Clinical Research Professor.

The costs of publication of this article were defrayed in part by the payment of page charges. This article must therefore be hereby marked *advertisement* in accordance with 18 U.S.C. Section 1734 solely to indicate this fact.

Note: Presented in part at the United States and Canadian Academy of Pathology Annual Meeting, Vancouver, BC, Canada, March, 2004; M. A. Rubin and K. J. Pienta share senior authorship.

Requests for reprints: Rajal B. Shah, Department of Pathology, University of Michigan, 2G332 UH, 1500 East Medical Center Drive, Ann Arbor, MI 48109-0054. Phone: (734) 936-6776; Fax: (734) 763-4095; E-mail: rajshah@umich.edu.

Table 1 *Clinical characteristics of 30 rapid autopsies*

Case no.	Age at death (year)	Gleason score at initial diagnosis	Treatment *	Months treated with hormones prior to chemotherapy	Months hormone refractory
1	77	9	R, H, C	23	26
2	59	Metastasis †	H, C, X	12	21
3	53	Metastasis †	H, C, X	0	20
4	71	4 ‡	R, H, C	24	13
5	54	9	R, H, C	36	7
6	71	6 ‡	P, R, H, C	30	2
7	65	9	R, H, C	31	34
8	68	Unknown	P, R, H, C	51	16
9	68	7 ‡	P, R, H, C	144	21
10	78	Unknown	R, H, C	24	12
11	67	8	R, H, C	12	5
12	79	7	H, C	42	19
13	71	Unknown	P, R, H, C	120	13
14	76	6	R, H, C	84	17
15	74	10	R, H, C	4	3
16	70	7	P, R, H, C	24	14
17	74	7	H, C, X	21	11
18	61	5 ‡	P, R, H, C	60	14
19	84	7	R, H, C, X	69	28
20	66	9	P, R, H, C, X	65	14
21	64	9	R, H, C	25	30
22	64	8	H, C, X	22	9
23	72	6	R, H, C	27	45
24	76	7	R, H, C, X	13	9
25	66	Unknown	H, X	42	0
26	76	Unknown	R, H, C, X	60	35
27	74	7	R, H, C	80	15
28	86	Unknown	P, H, C	119	61
29	77	8	R, H, C	102	8
30	71	9	H, C, X	13	16

* Treatment regimens: H, hormone ablation by bilateral orchiectomy and/or pharmacological blockage; C, chemotherapy; R, primary or salvage radiation; P, radical prostatectomy; X, palliative radiation.

† Initial presentation as metastasis outside prostate.

‡ Pathology slides not available for review.

the tested markers (0–100%). The final data were recorded in a Microsoft Excel datasheet and were used for statistical analysis.

Microarray Analysis (cDNA). The spotted cDNA microarrays used for the identification of differentially expressed genes in the rapid autopsy series have been previously described (6, 7). The cDNA arrays contained ~5,500 known, named genes from the Research Genetics human cDNA clone set, and >4,400 expressed sequence tags (7). The expression array data were analyzed with a Cluster and TreeView[8] to explore for relationships between samples (14).

Statistical Analysis. Regression tree was fitted with time from chemotherapy to death as response, and each immunohistochemistry marker percentage staining values was dichotomized according to the root node splitter from the fitted tree. Survival time was divided into >14.5 months and <14.5 months to represent good *versus* bad outcome, and 2 × 2 contingency table was generated to test the association between the outcome and maker staining levels. Exact test and linear regression were also performed with statistical software package (SAS Institute Inc., Cary, NC) to measure association between different clinical variables and immunomarkers with survival time.

RESULTS

Clinical Findings from 30 Rapid Autopsy Cases. Between September 1996 and November 2003, 30 rapid autopsies were performed on men who died of advanced hormone-refractory prostate cancer (Table 1). The median age at time of death was 71 years (range, 53–84 years). Twenty-eight men were initially diagnosed with clinically localized prostate cancer but developed widely disseminated disease after 5–10 years. Eight men underwent radical prostatectomy before receiving additional treatment and 17 men received external beam radiation as their primary treatment. Twenty-eight men received combination chemotherapy, and all underwent hormonal manipulation. Initial Gleason score was documented in 20 of 30 men and ranged from 4 to 10. The time that patients were treated with androgen deprivation ranged from 0 to 144 months. Patients survived in the hormone-refractory state (measured as time from first chemotherapy) from 0 to 61 months with a hormone-refractory median survival of 14.5 months.

Rapid Autopsy Findings. Widely disseminated prostate cancer was found in most cases. Bone (83%) was the commonest site of metastasis, followed by liver (66%), lymph nodes (63%), lungs (50%), soft tissues (40%), dura (26%), and adrenal glands (23%). A summary of the percentage distribution pattern of prostate cancer metastasis is presented in Fig. 1*A*. Six cases (20%) had predominantly skeleton system involvement; however, no cases presented with only bone involvement. Five cases (16%) presented with only visceral organ involvement (liver and/or lymph node) without grossly observable evidence of bone involvement. The prostate gland was present in 70% (21 of 30) of cases; of these, 6 cases demonstrated androgen therapy effect as has been previously described in primary prostate cancer (15). Residual tumor was identified in 20 of 21 cases, 8 cases had extensive disease with involvement of bladder and pelvic soft tissues, and 12 had low volume of disease.

Review of the histologic appearance of these metastatic prostate cancers revealed heterogeneous patterns with architectural patterns

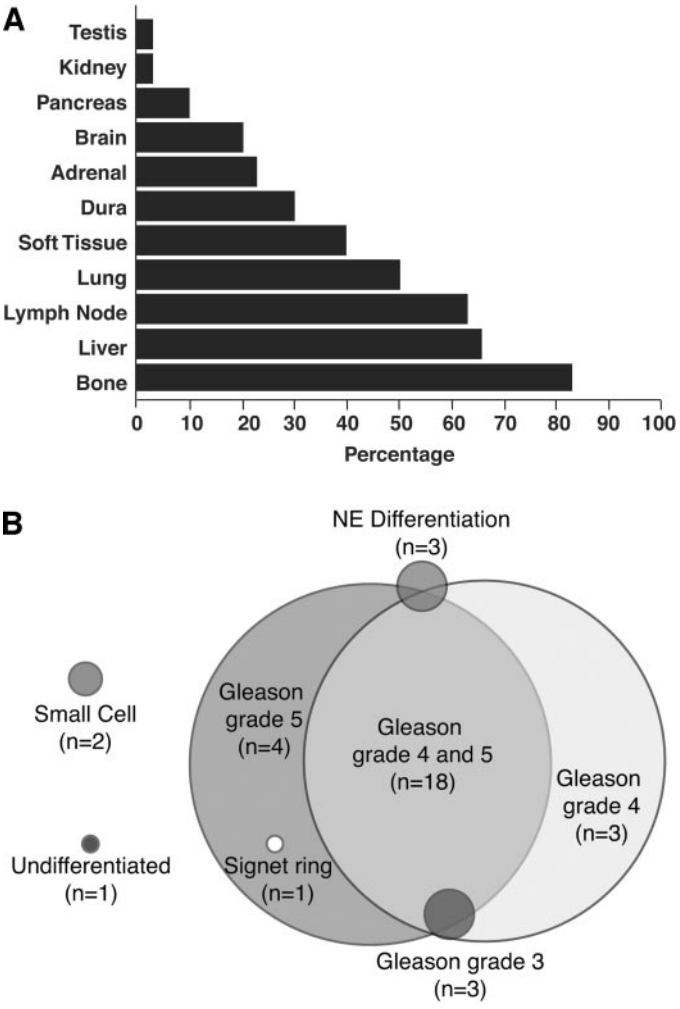

Fig. 1. *A*, distribution of hormone-refractory prostate cancer metastasis from 30 rapid autopsy cases performed at the University of Michigan. *B*, schematic overview of the distribution and overlap of the different histologic patterns identified in the cases from the rapid autopsy hormone-refractory metastatic prostate cancers (*NE*, neuroendocrine).

[8] http://www.microarrays.org.

Table 2 *Demonstration of the immunophenotype of hormone-refractory metastatic (met) prostate cancers in 30 rapid autopsy cases*

ID	No. of met sites	AR	AMACR	SYN	MIB-1	CGA	PSA	Morphology	Time from chemotherapy to death (months)
1	5	3.6 ± 2.8	17.7 ± 2.3	0.7 ± 0.1	5 ± 0.6	1.8 ± 3.8	79.6 ± 8.7	GP 5 + 4+NE	26
2	2	4.2 ± 2.5	7.5 ± 1.0	0.6 ± 3.3	8.4 ± 0.4	3.9 ± 1.6	24.1 ± 4.6	NE	21
3	8	44.3 ± 10.8	7.7 ± 2.1	0.2 ± 1.9	4.8 ± 0.9	1.5 ± 0.8	62.7 ± 14.4	GP4 + 3	20
4	2	23 ± 4.1	2.5 ± 0.3	0.8 ± 1.0	1.6 ± 0.3	0.8 ± 0.5	28.1 ± 5.0	GP 5	13
5	5	21.8 ± 2	10.7 ± 0.7	0.3 ± 1.5	3.3 ± 0.3	3 ± 0.4	16.5 ± 2.8	GP 5	7
6	3	14.1 ± 3.7	30.8 ± 2.9	3.8 ± 1.0	1.3 ± 0.3	3.9 ± 0.6	49 ± 6.3	GP 5 + 4	2
7	2	NA	1.9 ± 0.3	20.7 ± 2.2	2.8 ± 0.3	8.4 ± 0.7	73.8 ± 1.7	GP 4	34
8	3	8.3 ± 0.0	37.7 ± 3.7	1.4 ± 0.0	7.4 ± 0.2	13.9 ± 0.2	38 ± 6.1	GP 5 + 4	16
9	1	20 ± 1.2	30.4 ± 2.5	12 ± 0.6	3.4 ± 0.1	5.1 ± 0.1	66.6 ± 1.7	GP 4 + 3	21
10	3	16.9 ± 2.6	15.6 ± 2.2	19.9 ± 1.1	6.5 ± 0.7	10 ± 0.4	31.1 ± 4.0	GP 5 + 4	12
11	1	NA	11.4 ± 0.5	7 ± 0	14.3 ± 1.9	2.4 ± 0.1	3.3 ± 0.1	Undifferentiated	5
12	3	0.3 ± 0.2	2.4 ± 0.2	0.4 ± 0.1	2.1 ± 0.3	1.1 ± 0.1	61.9 ± 0.2	GP 5 + 4	19
13	4	NA	0.6 ± 0.1	0.4 ± 0.2	5.2 ± 1.2	2 ± 0.5	49.8 ± 2.8	GP 5 + 4+NE	13
14	6	0.7 ± 2.7	23.9 ± 4.9	0.7 ± 2.1	2 ± 0.6	1.2 ± 1.3	83.5 ± 10.1	GP 5 + 4	17
15	2	56.3 ± 2.8	17.2 ± 4	0.4 ± 0.2	1.7 ± 0.7	0.7 ± 0.3	98.1 ± 2.8	GP 5 + 4	5
16	4	85.6 ± 4.7	16 ± 2.5	0.7 ± 0.2	14.8 ± 1.3	1.5 ± 0.2	96.9 ± 2.2	GP 5	14
17	4	0.4 ± 0.2	5.7 ± 2.4	8.1 ± 2.4	4.9 ± 0.5	4.1 ± 1.2	2 ± 2.7	GP 5 + 4+3	11
18	2	75 ± 5.4	3.8 ± 0.2	0.2 ± 0.01	5.1 ± 0.2	1.7 ± 1.0	58.7 ± 1.7	GP 4	14
19	3	43 ± 7	4.1 ± 2.7	2.3 ± 1.0	4.2 ± 0.4	0.9 ± 0.7	87.1 ± 2.0	GP 5	28
20	4	23.9 ± 5	0.4 ± 0.1	0.4 ± 1.5	2.3 ± 0.2	8.8 ± 1.2	2.1 ± 2.6	GP 5 + 4	14
21	3	0.2 ± 1.3	3.1 ± 0.3	0.9 ± 0.9	1.8 ± 0.3	1.9 ± 0.6	51.2 ± 4.4	GP 5 + 4	30
22	4	0.3 ± 1.3	3.6 ± 0.9	1.6 ± 4.5	8.8 ± 1.6	5.5 ± 1.6	4.1 ± 2.8	Small cell	9
23	3	52.4 ± 0.4	22.7 ± 3.9	7.8 ± 1.6	3.2 ± 1.0	5 ± 1.1	58.1 ± 5.1	GP 5 + 4	45
24	6	4.4 ± 3.6	8.2 ± 1.2	3.4 ± 3.4	7.5 ± 2.0	18 ± 4.6	10 ± 10.0	Small cell	9
25	2	32.9 ± 4.2	10.5 ± 0.6	1.2 ± 0.3	11.9 ± 0.1	1.5 ± 0.1	3.3 ± 6.3	GP 5 + 4	0
26	5	21.7 ± 1.9	15.6 ± 4.7	1.8 ± 1.9	7.8 ± 1.9	3.6 ± 0.7	19.9 ± 5.3	GP 5 + 4	35
27	1	29.2 ± 3.7	8 ± 0.3	6.9 ± 0.6	2.3 ± 0.1	7.3 ± 0.9	40.6 ± 2.1	GP 5 + 4	15
28	4	83.4 ± 8.3	16.7 ± 4.3	0.2 ± 1.6	5.9 ± 1.0	1.1 ± 0.8	64.5 ± 6.5	GP 5 + 4	61
29	1	47.3 ± 0.0	13.3 ± 0	15.3 ± 1.6	4.8 ± 0.3	6.8 ± 0.0	33.4 ± 2.5	GP 5 + 4	8
30	7	87 ± 7.7	5.8 ± 2.7	0.5 ± 1.9	4.6 ± 1.0	1.9 ± 0.9	8.5 ± 5.8	GP 5 + 4	16

NOTE. Median % staining (± SEM) of all metastatic samples from 30 rapid autopsy cases evaluated with different immunomarkers.
Abbreviations: ID, identification number; GP, Gleason pattern; NE, neuroendocrine; NA, Not available.

similar to primary prostate cancers as described by Gleason (16). Although Gleason grading in a clinical setting is not recommended for metastatic tumors (17), we nevertheless applied the Gleason grades to use a system that is well known to practicing pathologists. The distribution and overlap of different histologic patterns identified in these cases are schematically demonstrated in Fig. 1*B* and summarized in Table 2. Four cases had uniform tumor morphology at all sites, growing in solid sheets and nests with or without comedonecrosis, resembling Gleason grade 5 (Fig. 2*A* and *B*). Three cases demonstrated uniform morphology at all sites, with tumors growing in a confluent cribriform glandular pattern resembling Gleason grade 4 (Fig. 2*C*). The majority of cases (18 cases) had tumors with a mixture of the above two growth patterns resembling a mixture of Gleason grades 4 and 5. Three cases demonstrated neuroendocrine differenti-

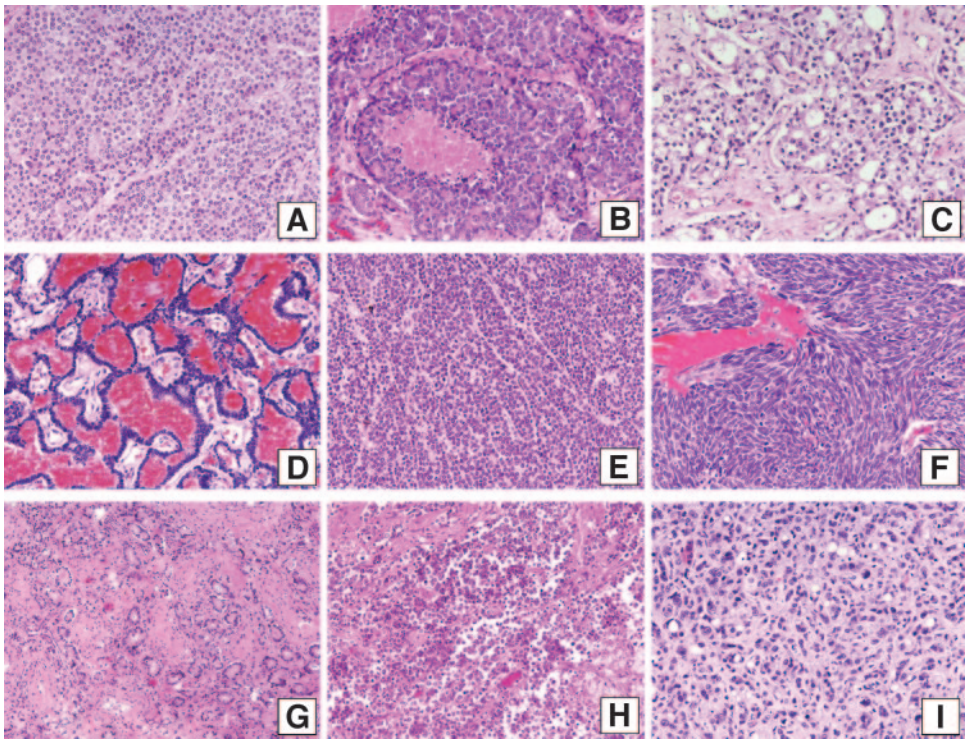

Fig. 2. *A–I*, hematoxylin and eosin stain. Histologic spectrum of treated metastatic prostate cancer: Solid sheets and nests of uniform tumor cells without (*A*, ×200), and with comedonecrosis (*B*, ×200) similar to Gleason grade 5, confluent cribriform glandular pattern of tumor similar to Gleason grade 4 (*C*, ×200), Neuroendocrine differentiation characterized by growth pattern of ribbons, trabaculae, and nests with uniform round nuclei, high N:C ratio, and salt and pepper chromatin (*D–E*, ×200), small-cell carcinoma, characterized by spindling and molding of the nuclei and high mitotic activity (*F*, ×400), uniform tumor cells with well-formed glands similar to Gleason grade 3 (*G*, ×200), tumor cells demonstrating poor cohesion with an undifferentiated growth pattern (*H*, ×400), and tumor with signet ring cell differentiation (*I*, ×200).

ation characterized by tumor growing in nests, trabaculae, and ribbons with uniform round nuclei, high N:C ratio, and salt and pepper chromatin (Fig. 2*D* and *E*). Only one of these three cases was seen as pure growth pattern, whereas in the remaining two cases, neuroendocrine differentiation was seen in combination with Gleason grade 5 pattern. Two cases had tumors with small-cell neuroendocrine carcinoma, similar to oat-cell carcinoma of the lung, characterized by spindling, crushing, and molding of the nuclei and high mitotic activity (Fig. 2*F*). Three cases had well-formed glands resembling Gleason grade 3 at some metastatic sites in addition to other growth patterns (three cases; Fig. 2*G*). In one case, metastatic tumors demonstrated poor cohesion with an undifferentiated growth pattern (Fig. 2*H*), and another case demonstrated focal signet ring cell differentiation (Fig. 2*I*) in addition to growth pattern of Gleason grade 5. The wide range of these varied histologic patterns is summarized and illustrated in Fig. 2 and Table 2. The distribution and overlap of different histologic patterns identified in these cases are schematically demonstrated in Fig. 1*B*. In one case, focal sarcomatoid differentiation was present only within the prostate site. Focal to diffuse nuclear pleomorphism within tumor cells was seen in 40% of cases, the remaining cases showed round-to-oval uniform nuclei often with prominent nucleoli, a bland cytology typical of prostate cancer.

Choice of Immunomarkers. Previous work by our group and others have described the immunophenotype of hormone-refractory metastatic prostate tumors (7, 8, 18–20). One limitation of our previous work has been the subjective manner in which protein expression was reported. Therefore, to attempt to provide more quantitative results and to study potential heterogeneity, we used the Chroma vision ACIS II system for the evaluation of several prostate cancer immunomarkers including PSA, AR, CGA, SYN, MIB-1, and AMACR. PSA was chosen because of its common use as a surrogate marker in the treatment of metastatic disease. AR was chosen because of its importance in understanding the development of androgen-independent disease. CGA and SYN were chosen to explore the concept of neuroendocrine differentiation in androgen-independent disease. MIB-1 was chosen as a proliferation marker. AMACR, a new molecular marker, has previously been shown to be a highly sensitive marker for clinically localized prostate cancer and colorectal cancer (3, 21). Our group recently demonstrated that AMACR expression is down-regulated in hormone-refractory metastatic prostate cancer, is androgen independent, and is likely related to tumor differentiation (22).

Immunophenotype of Prostate Cancer in Different Patients. The results are summarized in Table 2. The data present the median percentage staining with the range of the immunomarkers across all patients according to tissue site as present on the tissue microarray. All of the immunomarkers demonstrated considerable heterogeneity across disease sites. PSA expression was seen to vary for the percentage of PSA-positive cells with median expression of 39.3 (range, 0.3 to 99.44; SEM, 34.5; Table 2; Fig. 3). Consistent with its role as a transcription factor, AR was localized in nuclei. AR expression varied across tumor samples with 31% (83 of 265) of tumor samples expressing >50% AR and 41.5% (100 of 265) expressing <10% AR. Overall expression of AR was down-regulated with median AR expression of 20.04% (range, 0–100%, SEM, 34.28; Table 2; Fig. 3). The intensity of AMACR expression varied among the metastatic tumors; the median percentage of positive tumor cells was 8.18% (range, 0.19–71.97%; SEM, 14.58). The median MIB-1 expression was 4.55% (range, 0.25–26%; SEM, 4.61). CGA and SYN were infrequently observed in these metastatic prostate cancer cases, as we have reported previously (8). The median percentage of metastatic tumor cells demonstrating either CGA or SYN protein expression was 2.23% (range, 0.21–62.51; SEM, 7.55) and 0.83% (range, 0–49.11%; SEM, 8.21), respectively. Cases with neuroendocrine/small-cell morphology usually demonstrated neuroendocrine expression. We investigated whether any of the immunomarkers were predictive of survival time from the initiation of chemotherapy to death. Patients with a PSA median expression >50% demonstrated a significantly better survival than those with <50% expression ($P < 0.03$).

Immunophenotype of Prostate Cancer in the Same Patient. Having demonstrated the marked variation of immunomarkers in different organ sites and patients, we next investigated the expression of AR and PSA in tissue sites within the same patient. Tables 3 and 4 demonstrate the results for four different representative patients. Results are present as the median percentage staining. A range is given if there was more than one sample from that given site in a patient. All of the patients demonstrated marked differences in AR expression between different tissue sites (2- to 50-fold; Table 3). There was no pattern to the differences in AR expression between the different organ sites that could be distinguished, and this was true across all patients. Perhaps most striking was that several patients demonstrated a high amount of AR staining, although they were no longer responding to androgen-deprivation therapy. PSA expression also varied widely between tissue sites and, sometimes, even within the same tissue site of a patient (Table 4). For example, Case 30 demonstrated a range of PSA expression from a median of 3.03 in the prostate to a median of 60.61 in the bone, but the range of expression in the bone itself ranged from 14.67 to 77.86.

Expression Array Analysis of Different Metastatic Tissues. We next sought to determine whether the heterogeneity in histology and phenotype was mirrored by heterogeneity in gene expression. With expression array data that we have previously generated (6–8), we performed hierarchical clustering of the 16 metastatic samples from six cases in the rapid autopsy series. The metastatic adenocarcinoma samples were highly heterogeneous (Fig. 4). Only two metastases from a patient with small-cell histology demonstrated comparable cDNA expression results (Fig. 4). With the ONCOMINE database, we

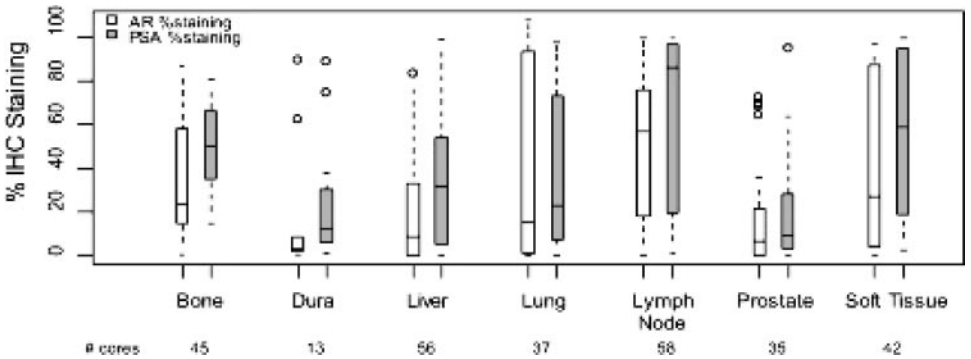

Fig. 3. Error bar graphs demonstrating variation of PSA and AR protein expression across the metastatic sites from 30 rapid autopsy cases. (*IHC*, immunohistography.)

Table 3 *Androgen receptor staining across metastatic sites for rapid autopsy (RA) cases 3, 14, 24, and 30*

Metastatic tissue	RA case 3	RA case 14	RA case 24	RA case 30
Adrenal	74.28 (64.4–78.93)			
Bone	22.66 (22.66–22.66)			81.07 (75.74–86.4)
Bladder				89.34 (88.54–96.65)
Dura	33.59 (5.17–62.01)		5.45 (1.86–9.04)	
Liver	46.22 (18.8–83.1)	0.48 (0.41–1.78)	2.28 (0.05–7.14)	
Lung	23.67 (15.41–27.4)	0.18 (0.1–0.22)	13.03 (5.64–41.95)	96.89 (85.49–99.56)
Lymph node	70.81 (40.78–94.65)		0.06 (0.06–0.06)	99.38 (99.01–99.58)
Meninges		0.73 (0.64–0.81)	0.01 (0–0.01)	68.93 (18.31–72.12)
Prostate	12.23 (3.7–13.61)	1.81 (1.29–2.33)		47.83 (16.3–87.04)
Soft tissue		19.99 (0.49–29.08)		
Testis	10.7 (10.7–10.7)			

NOTE. Median % staining of AR (range). There is one metastatic site less for cases 14 and 24 each of AR staining because of missing values. Tables 3 and 4 demonstrate heterogeneity in PSA and AR protein expression of metastatic sites in the same patient.

found that these tumors exhibited a similar expression pattern as small-cell lung cancer (23).

DISCUSSION

Autopsy series have been a valuable part of understanding the natural history of diseases, including prostate cancer (24–29). This study underscores the continued importance of the autopsy in modern medicine. It demonstrates that metastatic cancer is a group of diseases and needs to be treated as such and emphasizes the importance of obtaining metastatic tissue to understand the biology of prostate cancer. It is a widespread belief that prostate cancer metastasizes to osseous sites but rarely to visceral organs. Three groups (*i.e.,* University of Michigan, Ann Arbor, MI; University of Washington, Seattle, Washington; and Johns Hopkins University, Baltimore, Maryland) have developed rapid autopsy programs with the goal of procuring metastatic osseous and nonosseous prostate cancer samples for research purposes (2, 20). Our data and those of others demonstrate that prostate cancer commonly metastasizes to lymph nodes, liver, lung, adrenal, and dura sites in addition to the bone (20, 24). The MIB-1 data confirm the work of others in demonstrating the slow doubling time of prostate cancer, which suggests that the cancer develops in multiple sites over a long period of time (30, 31). These data also have implications for developing therapy because treatment based on using agents that act on cells with a rapid doubling time may not be effective in androgen-independent prostate cancer. The low rate of effectiveness of traditional chemotherapy agents in prostate cancer appears to reflect this finding.

We, as well as others, have identified several genes that are differentially expressed in primary *versus* metastatic disease (6, 7, 32). By definition, these analyses are designed to find potential similarities between samples at a similar disease stage and compare the two groups. Whereas these studies have identified several potential biomarkers, they were also remarkable for the amount of heterogeneity and overlap between primary and metastatic samples. To date, metastatic prostate tissue samples from the same patient and between patients have not been systematically been analyzed in an attempt to quantify this heterogeneity and to determine whether it may be important. Our data demonstrate that there are substantial differences in the genotype and phenotype of metastatic prostate cancer between patients and within the same patient. The data in Tables 2, 3, and 4, as well as in Fig. 3 demonstrate this heterogeneity when comparing metastatic sites. We did not investigate heterogeneity within individual metastatic sites by comparing multiple biopsies from a given site; however, it seems likely that heterogeneity would have been revealed at that level also. This will be the subject of future studies.

Normal prostate tissue and virtually all primary prostate cancer have been found to uniformly express AR; however, information of AR expression in hormone-refractory prostate cancer is limited (33). Our study demonstrates heterogeneity in AR expression with frequent AR-positive and AR-negative tumor populations between and within the same patient (Tables 2 and 3). In this study, overall AR expression is down-regulated in hormone-refractory prostate cancer, with 41.5% of tumor samples demonstrating $<10\%$ of AR, which suggests that, in such cases, an alternate AR bypass mechanism may also be important in the progression of androgen independence (34). However, the majority of patients still express substantial amounts of AR although they have undergone long-term androgen ablation. Because intracellular AR, a ligand-dependent transcription activator mediates androgen action, abnormalities in AR are believed to play an important role in the progression of prostate cancer (34–36). Chen *et al.* (37) have recently demonstrated that the AR in androgen-independent prostate cancer can still be active and fueled by submicromolar amount of testosterone. Our present study supports the observation that the AR still may play a central role in the biology of what has been traditionally termed "androgen-independent" disease.

Another clinically significant finding of this study is the low frequency of neuroendocrine phenotype in prostate cancer patients. It has been suggested that most androgen-independent prostate cancer has a neuroendocrine phenotype, and investigators have reported a correlation between the percentage of neuroendocrine expression with

Table 4 *Prostate-specific antigen staining across metastatic sites for rapid autopsy (RA) cases 3, 14, 24, and 30*

Metastatic tissue	RA case 3	RA case 14	RA case 24	RA case 30
Adrenal	98.54 (98.42–98.89)			
Bone	47.86 (44.63–51.08)	64.92 (57.03–72.82)	61.62 (61.62–61.62)	60.61 (14.67–77.86)
Bladder				2.84 (2.02–3.61)
Dura	47.27 (6.25–88.3)		2.27 (1.43–2.33)	5.84 (5.84–5.84)
Liver	39.41 (5.72–77.58)	96.03 (94.14–97.58)	20.14 (5.85–39.3)	
Lung	28.93 (7.87–49.09)	83.42 (12.43–97.61)	2.74 (1.47–95.45)	3.59 (0.34–14.07)
Lymph node	97 (86.18–98.29)		8.57 (8.57–8.57)	9.1 (8.53–13.27)
Meninges		41.65 (31.83–51.47)		
Prostate	61.67 (57.49–63.7)	4.27 (3.59–4.95)	13.05 (11.95–14.16)	3.03 (1.2–5.22)
Soft tissue		93.77 (83.49–98.61)		20.91 (3.91–39.04)
Testis	97.79 (97.79–97.79)			

NOTE. Median % staining of PSA (range). Tables 3 and 4 demonstrate heterogeneity in PSA and AR protein expression of metastatic sites in the same patient.

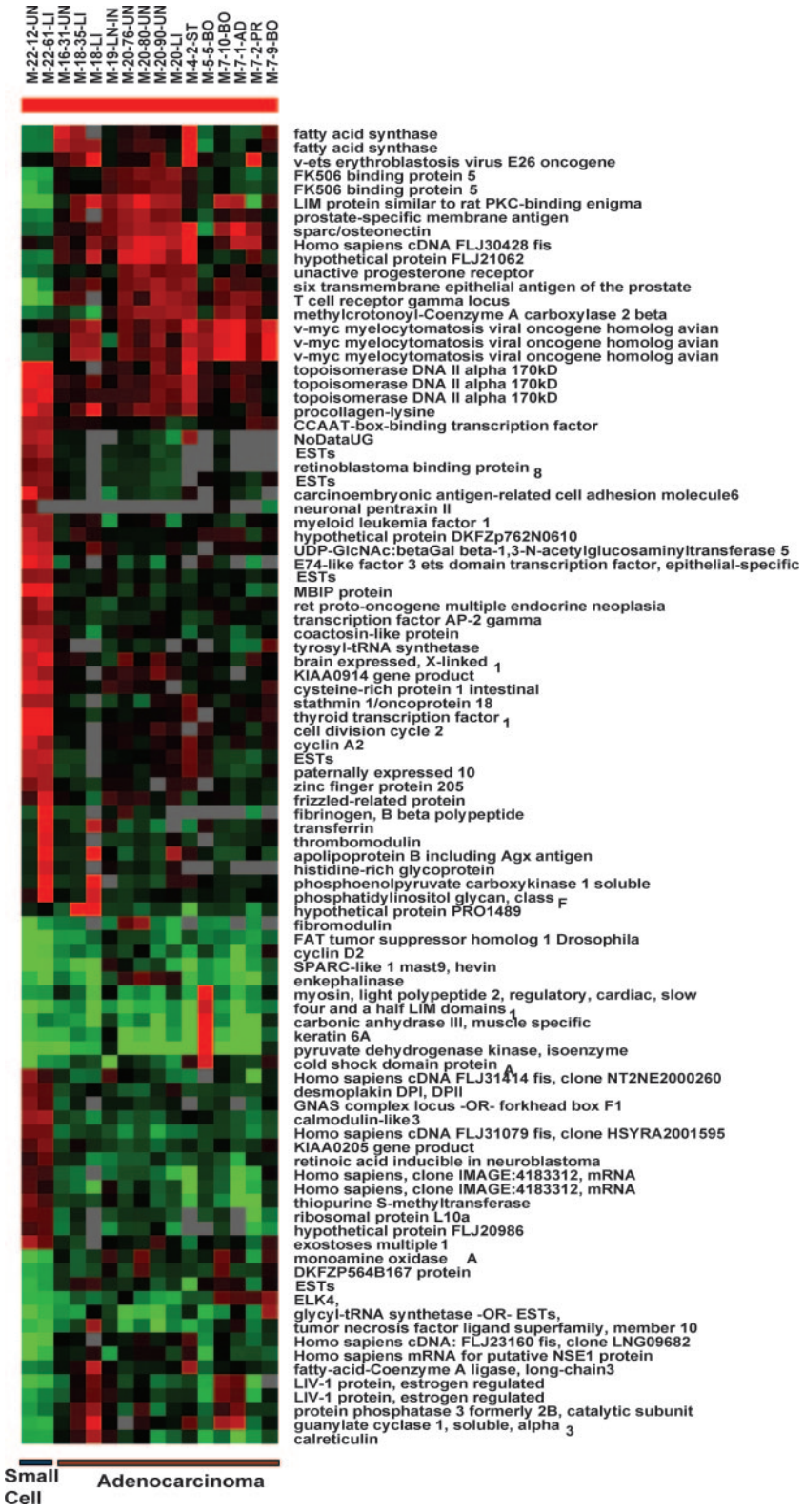

Fig. 4. Hierarchical clustering of 16 hormone-refractory metastatic prostate tumors from the rapid autopsy series demonstrates a small subset of genes that were specifically overexpressed in the small-cell phenotype (*lower left*) but not in the more typical glandular adenocarcinoma (see Discussion for details).

tumor progression and an adverse outcome (8, 20, 38, 39). Our data, as well as those of others, especially from the University of Washington, Seattle, suggest that this is not the case (20). In our series, only three patients demonstrated neuroendocrine phenotype by histology (two with pure small-cell histology and one with pure neuroendocrine differentiation but not reaching the threshold of small-cell carcinoma). Immunostaining for SYN and CGA was considerably variable and did not correlate with clinical outcome in the androgen-independent patients (as measured from the time of first chemotherapy).

We have extensively used these tumor samples from the rapid autopsy for research directed at understanding prostate cancer progression. Initial expression array analysis was critical in the identification of prostate- and cancer-specific genes such as *Hepsin*, *EZH2*, *MTA1*, and *TPD52*. (6, 7, 40) This initial work grouped all of the

hormone-refractory metastatic prostate cancer samples together for purposes of analysis and compared them with primary cancers as well as with normal tissue. These analyses were valuable in that they picked out dominant genes that were expressed differently over a majority of different tumor stages; however, these studies were not done by laser-capture microdissection and, therefore, did not take into account the heterogeneity of the tissues at similar stages. After review of the wide spectrum of histology in this study, we also questioned whether there was heterogeneity of gene expression when comparing metastatic tissue in androgen-independent disease. To our knowledge, this type of analysis, comparing metastatic samples against themselves, has not been done previously. We performed hierarchical clustering of 16 tumor samples from eight rapid autopsy cases. One case with two samples from two different sites had small-cell morphology. Whereas a few genes were differentially expressed in the majority of the metastatic sites including topoisomerase IIα, M_r 170,000 and procollagen-lysine, the majority of metastases did not share a similar gene expression pattern. These data demonstrate that the metastases share more differences than similarities in gene expression when compared with each other. These data were previously obscured when the metastases were used as part of larger arrays comparing normal and primary cancers with metastatic tissue. When we viewed the 95 most substantially differentially expressed genes, there were clusters of genes that were overexpressed only in the small-cell metastatic samples (Fig. 4). When small-cell prostate cancer does occur, it seems to have the genotypic pattern of small-cell lung cancer. With ONCOMINE, we were able to interrogate other over-60-expression array datasets that contained information on these differentially expressed genes (23). Multiple genes, including *TTF-1*, *PLOD2*, *TOP2A*, *Cyclin A2*, *CDC2*, *RBBP8*, and *GNAS*, found to be overexpressed in the two samples from a metastatic small-cell cancer of the prostate have all been previously identified as being significantly overexpressed in small-cell cancers of lung as compared with benign lung tissue as demonstrated by the adjusted *P*-values with ONCOMINE (40–43).

Previous studies have demonstrated the value of using PSA immunohistochemistry in the diagnosis of metastatic prostate cancer (44, 45). As previously noted by Stein et al. (45), the majority of end-stage prostate cancers retain PSA expression if all tumor samples are evaluated; however PSA expression is quite variable when individual tumor samples are evaluated (Tables 2, 4). There seemed to be no correlation between AR expression and PSA expression, which suggests that PSA expression may be driven by non-AR mechanisms in late-stage prostate cancer. We noted that patients with a median PSA staining of >50% had a longer survival in the androgen-independent setting than those with <50% staining. Roudier *et al.* (20) also found that that tumors with >50% of sites with >50% of cells expressing PSA were significantly associated with longer survival.

In conclusion, it is of note that no single biomarker or group of biomarkers has yet been identified that can successfully predict disease recurrence 100% of the time. Although studies have tried to identify subsets of genes that characterize the metastatic phenotype, these, by definition, ignore the heterogeneity of metastatic cancer (6, 7, 32). We demonstrate that end-stage hormone-refractory metastatic prostate cancer is a heterogeneous group of diseases. Understanding this heterogeneity is key to understanding prostate cancer progression and to guiding the development of future treatment paradigms.

ACKNOWLEDGMENTS

We thank the patients and their family members who, through their generous participation in this tissue donor program, have facilitated the study of advanced prostate cancer; Robin Kunkel for assistance in preparing figures; Srilakshmi Bhagavathula for assistance in preparation of the database; and Dr. Lakshmi Priya Kunju for her participation in the performance of rapid autopsy cases.

REFERENCES

1. Jemal A, Murray T, Samuels A, Ghafoor A, Ward E, Thun MJ. Cancer statistics, 2003. CA Cancer J Clin 2003;53:5–26.
2. Rubin MA, Putzi M, Mucci N, et al. Rapid ("warm") autopsy study for procurement of metastatic prostate cancer. Clin Cancer Res 2000;6:1038–45.
3. Rubin MA, Zhou M, Dhanasekaran SM, et al. alpha-Methylacyl coenzyme A racemase as a tissue biomarker for prostate cancer. JAMA 2002;287:1662–70.
4. Sun YX, Wang J, Shelburne CE, et al. Expression of CXCR4 and CXCL12 (SDF-1) in human prostate cancers (PCa) in vivo. J Cell Biochem 2003;89:462–73.
5. Xin W, Rhodes DR, Ingold C, Chinnaiyan AM, Rubin MA. Dysregulation of the annexin family protein family is associated with prostate cancer progression. Am J Pathol 2003;162:255–61.
6. Varambally S, Dhanasekaran SM, Zhou M, et al. The polycomb group protein EZH2 is involved in progression of prostate cancer. Nature (Lond) 2002;419:624–29.
7. Dhanasekaran SM, Barrette TR, Ghosh D, et al. Delineation of prognostic biomarkers in prostate cancer. Nature (Lond) 2001;412:822–26.
8. Mucci NR, Akdas G, Manely S, Rubin MA. Neuroendocrine expression in metastatic prostate cancer: evaluation of high throughput tissue microarrays to detect heterogeneous protein expression. Hum Pathol 2000;31:406–14.
9. Rubin MA, Dunn R, Strawderman M, Pienta KJ. Tissue microarray sampling strategy for prostate cancer biomarker analysis. Am J Surg Pathol 2002;26:312–9.
10. Kononen J, Bubendorf L, Kallioniemi A, et al. Tissue microarrays for high-throughput molecular profiling of tumor specimens. Nat Med 1998;4:844–7.
11. Hilbe W, Gachter A, Duba HC, et al. Comparison of automated cellular imaging system and manual microscopy for immunohistochemically stained cryostat sections of lung cancer specimens applying p53, ki-67 and p120. Oncol Rep 2003; 10:15–20.
12. Wang S, Saboorian MH, Frenkel EP, et al. Assessment of HER-2/neu status in breast cancer. Automated Cellular Imaging System (ACIS)-assisted quantitation of immunohistochemical assay achieves high accuracy in comparison with fluorescence in situ hybridization assay as the standard. Am J Clin Pathol 2001;116:495–503.
13. Bauer KD, de la Torre-Bueno J, Diel IJ, et al. Reliable and sensitive analysis of occult bone marrow metastases using automated cellular imaging. Clin Cancer Res 2000; 6:3552–9.
14. Eisen MB, Spellman PT, Brown PO, Botstein D. Cluster analysis and display of genome-wide expression patterns. Proc Natl Acad Sci USA 1998;95:14863–8.
15. Reuter VE. Pathological changes in benign and malignant prostatic tissue following androgen deprivation therapy. Urology 1997;49(Suppl):16–22.
16. Gleason D. Classification of prostate carcinoma. Cancer Chemother Rep 1966;50: 125–8.
17. Amin MB, Grignon DJ, Humphrey PA, Srigley JR. Gleason grading of prostate cancer: a contemporary approach. 1st ed. Philadelphia: Lippincott Williams and Wilkins; 2003. p. 116.
18. Rubin MA, Mucci NR, Figurski J, Fecko A, Pienta KJ, Day ML. E-cadherin expression in prostate cancer: a broad survey using high-density tissue microarray technology. Hum Pathol 2001;32:690–7.
19. Zhou M, Shah R, Shen R, Rubin MA. Basal cell cocktail (34betaE12 + p63) improves the detection of prostate basal cells. Am J Surg Pathol 2003;27:365–71.
20. Roudier MP, True LD, Higano CS, et al. Phenotypic heterogeneity of end-stage prostate carcinoma metastatic to bone. Hum Pathol 2003;34:646–53.
21. Zhou M, Chinnaiyan AM, Kleer CG, Lucas PC, Rubin MA. Alpha-Methyl-CoA racemase: a novel tumor marker over expressed in several human cancers and their precursor lesions. Am J Surg Pathol 2002;26:926–31.
22. Kuefer R, Varambally S, Zhou M, et al. alpha-Methylacyl-CoA racemase: expression levels of this novel cancer biomarker depend on tumor differentiation. Am J Pathol 2002;161:841–8.
23. Rhodes DR, Yu J, Shanker K, et al. ONCOMINE: a cancer microarray database and data-mining platform. Neoplasia 2004;6:1–6.
24. Bubendorf L, Schopfer A, Wagner U, et al. Metastatic patterns of prostate cancer: an autopsy study of 1,589 patients. Hum Pathol 2000;31:578–83.
25. Billis A. Latent carcinoma and atypical lesions of prostate. An autopsy study. Urology 1986;28:324–9.
26. Gatling RR. Prostate carcinoma: an autopsy evaluation of the influence of age, tumor grade, and therapy on tumor biology. South Med J 1990;83:782–4.
27. Sakr WA, Grignon DJ, Crissman JD, et al. High grade prostatic intraepithelial neoplasia (HGPIN) and prostatic adenocarcinoma between the ages of 20–69: an autopsy study of 249 cases. In Vivo 1994;8:439–43.
28. Stemmermann GN, Nomura AM, Chyou PH, Yatani R. A prospective comparison of prostate cancer at autopsy and as a clinical event: the Hawaii Japanese experience. Cancer Epidemiol Biomark Prev 1992;1:189–93.
29. Silvestri F, Bussani R, Pavletic N, Bassan F. Neoplastic and borderline lesions of the prostate: autopsy study and epidemiological data. Pathol Res Pract 1995;191:908–16.
30. Berges RR, Vukanovic J, Epstein JI, et al. Implication of cell kinetic changes during the progression of human prostatic cancer. Clin Cancer Res 1995;1:473–80.
31. Pinski J, Parikh A, Bova GS, Isaacs JT. Therapeutic implications of enhanced G(0)/G(1) checkpoint control induced by coculture of prostate cancer cells with osteoblasts. Cancer Res 2001;61:6372–6.
32. Ramaswamy S, Ross KN, Lander ES, Golub TR. A molecular signature of metastasis in primary solid tumors. Nat Genet 2003;33:49–54.

33. Hobisch A, Culig Z, Radmayr C, Bartsch G, Klocker H, Hittmair A. Distant metastases from prostatic carcinoma express androgen receptor protein. Cancer Res 1995; 55:3068–72.
34. Jenster G. The role of the androgen receptor in the development and progression of prostate cancer. Semin Oncol 1999;26:407–21.
35. Culig Z, Klocker H, Bartsch G, Hobisch A. Androgen receptors in prostate cancer. Endocr-Relat Cancer 2002;9:155–70.
36. Suzuki H, Ueda T, Ichikawa T, Ito H. Androgen receptor involvement in the progression of prostate cancer. Endocr-Relat Cancer 2003;10:209–16.
37. Chen CD, Welsbie DS, Tran C, et al. Molecular determinants of resistance to antiandrogen therapy. Nat Med 2004;10:33–9.
38. Aprikian AG, Cordon-Cardo C, Fair WR, et al. Neuroendocrine differentiation in metastatic prostatic adenocarcinoma. J Urol 1994;151:914–9.
39. Bostwick DG, Qian J, Pacelli A, et al. Neuroendocrine expression in node positive prostate cancer: correlation with systemic progression and patient survival. J Urol 2002;168:1204–11.
40. Rhodes DR, Barrette TR, Rubin MA, Ghosh D, Chinnaiyan AM. Meta-analysis of microarrays: interstudy validation of gene expression profiles reveals pathway dysregulation in prostate cancer. Cancer Res 2002;62:4427–33.
41. Fabbro D, Di Loreto C, Stamerra O, Beltrami CA, Lonigro R, Damante G. TTF-1 gene expression in human lung tumours. Eur J Cancer 1996;32A:512–7.
42. Harlamert HA, Mira J, Bejarano PA, et al. Thyroid transcription factor-1 and cytokeratins 7 and 20 in pulmonary and breast carcinoma. Acta Cytol 1998;42: 1382–8.
43. Agoff SN, Lamps LW, Philip AT, et al. Thyroid transcription factor-1 is expressed in extrapulmonary small cell carcinomas but not in other extrapulmonary neuroendocrine tumors. Mod Pathol 2000;13:238–42.
44. Shah NT, Tuttle SE, Strobel SL, Gandhi L. Prostatic carcinoma metastatic to bone: sensitivity and specificity of prostate-specific antigen and prostatic acid phosphatase in decalcified material. J Surg Oncol 1985;29:265–8.
45. Stein BS, Vangore S, Petersen RO. Immunoperoxidase localization of prostatic antigens. Comparison of primary and metastatic sites. Urology 1984;24:146–52.

Androgen-Independent Prostate Cancer Is a Heterogeneous Group of Diseases: Lessons from a Rapid Autopsy Program

Rajal B. Shah, Rohit Mehra, Arul M. Chinnaiyan, et al.

Cancer Res 2004;64:9209-9216.